A Self-Consistent Approach for Calculating the Effective Hydraulic Conductivity of a Bimodal, Heterogeneous Medium

Sergey Pozdniakov
Faculty of Geology
Moscow State University
119899 Vorobiovy Gory, Moscow, Russia
Email sppozd@geol.msu.ru

Chin-Fu Tsang
Earth Sciences Division
Lawrence Berkeley National Laboratory
One Cyclotron Road, Berkeley, CA 94720, USA
Email cftsang@lbl.gov

ABSTRACT

In this paper, we consider an approach for estimating the effective hydraulic conductivity of a 3D medium with a binary distribution of local hydraulic conductivities. The medium heterogeneity is represented by a combination of matrix medium conductivity with spatially distributed sets of inclusions. Estimation of effective conductivity is based on a self-consistent approach introduced by Shvidler (1985). The tensor of effective hydraulic conductivity is calculated numerically by using a simple system of equations for the main diagonal elements. Verification of the method is done by comparison with theoretical results for special cases and numerical results of Desbarats (1987) and our own numerical modeling.

The method was applied to estimating the effective hydraulic conductivity of a 2D and 3D fractured porous medium. The medium heterogeneity is represented by a combination of matrix conductivity and a spatially distributed set of highly conductive fractures. The tensor of effective hydraulic conductivity is calculated for parallel- and random-oriented sets of fractures. The obtained effective conductivity values coincide with Romm's (1966) and Snow's (1969) theories for infinite fracture length. These values are also physically acceptable for the sparsely-fractured-medium case with low fracture spatial density and finite fracture length. Verification of the effective hydraulic conductivity obtained for a fractured porous medium is done by comparison with our own numerical modeling for a 3D case and with Malkovsky and Pek's (1995) results for a 2D case.

1 Introduction

The impact of heterogeneity on subsurface flow has been studied in recent years from several directions. One of the major research directions is the search for effective flow and transport parameters in heterogeneous medium. The main approaches and significant theoretical studies in this field have been summarized in Shvidler (1985), Dagan (1989), Gelhar (1993) and other publications. In theories that analyze flow in heterogeneous media, the spatial variation of the local hydraulic conductivity is typically described as a random field with a given statistical distribution (often assumed to be lognormal) and a covariance function. However, the internal structure of heterogeneous geological formations cannot always be realistically fitted to a theoretically convenient lognormal distribution (e.g., sand-shale aquifers, aquitards with highly contrasting hydraulic conductivity in the main facies, and fractured porous rocks). In these media, the connectivity of highly permeable bodies (e.g., sand, fractures) plays an important role in the overall hydraulic conductivity of the entire system (Fogg, 1986; Robinson, 1984).
Our goal is to (1) develop and verify a self-consistent method for calculating the effective hydraulic conductivity of a binary medium (i.e., a medium composed of two subsystems with arbitrarily contrasting hydraulic conductivity values), and (2) apply the results to a fractured porous medium.

The development is based on a general self-consistent approach to calculating the effective conductivity of composite materials, which for groundwater flow, was first applied by Shvidler (1985) and Dagan (1989), and later used by Rubin (1995) as well as Dagan and Lessoff (2001) for transport studies in binary systems.

In this paper, we analyze the effective hydraulic conductivity of a fractured porous system using a self-consistent approach, which allows the same approach to be applied to developing equations for the effective hydraulic conductivity of porous, fractured, and fractured porous media for many practically important cases.

2 Theory of Self-Consistent Approach

We consider a heterogeneous medium with a scalar, local hydraulic conductivity modeled by a binary field $K(\mathbf{x})$ where $\mathbf{x}=\{x_1,x_2,x_3\}$.The principal axes x_1 and x_2 are defined in the horizontal plane, whereas x_3 is the vertical direction. Consider the heterogeneity configuration shown in Figure 1. The matrix medium with intrinsic hydraulic conductivity k_m contains inclusions randomly distributed over space with hydraulic conductivity k_{inc}. Let us assume that each inclusion is an oblate spheroid with a coefficient of anisotropy $\varepsilon \le 1$; i.e., with the aspect ratio of vertical diameter λ_v to horizontal diameter λ_h of the spheroid less than one. The local Cartesian coordinates $\mathbf{x}_{inc}=\{x_{inc1},x_{inc2},x_{inc3}\}$ are at the center of each spheroidal inclusion and its main axes

have arbitrary directional cosines relative to the global system of **x** coordinates. Each inclusion has a given volume, but the volume of each inclusion is much less than the overall volume of the considered medium. Let p denote the volume fraction of all inclusions (i.e., the ratio of total volume of all inclusions to overall volume of the medium). Thus, for the described system, the hydraulic conductivity field K(**x**) takes on a value k_{inc} when the specified point is inside an inclusion; otherwise, it takes on the value k_m.

2.1 General Equations for Calculating Effective Conductivity

Consider the steady-state flow of groundwater. The local Darcy's flux **q** and hydraulic head h obey the system of equations:

$$\nabla \mathbf{q(x)} = 0 \quad \mathbf{q(x)} = -K(\mathbf{x})\mathbf{J} \quad \mathbf{J} = \nabla h \,. \tag{1}$$

Let us impose a hydraulic gradient $\mathbf{J}_{\text{ext}}$ on the external boundary of the medium. Then, the effective hydraulic conductivity satisfies Darcy's law for mean flux **Q**:

$$\mathbf{Q} = -\mathbf{K}_{\mathbf{ef}}\,\mathbf{J}_{\mathbf{ext}} \tag{2}$$

where $\mathbf{K}_{\text{ef}}$ is the tensor of effective hydraulic conductivity. The effective hydraulic conductivity for the heterogeneity model depends on the values of the intrinsic conductivities, the volume fraction of inclusions p, the coefficient of anisotropy ε, and the orientation of the inclusions in the medium. In the self-consistent approach for calculating effective properties, we assume that the hydraulic-head field inside of an inclusion depends on the properties of the inclusion and the homogeneous medium surrounding the inclusion. The properties surrounding the homogeneous medium can be either described by matrix conductivity k_m (Maxwell's method) or the effective conductivity.

Following Shvidler (1985), let us consider the system of flow and gradient balance equations:

$$\mathbf{K}_{ef}\,\mathbf{J}_{ext} = (1-p)k_m\mathbf{J}_m + pk_{inc}\mathbf{J}_{inc} \tag{3a},$$

$$\mathbf{J}_{ext} = (1-p)\mathbf{J}_m + p\mathbf{J}_{inc} \tag{3b},$$

where $\mathbf{J}_{\text{m}}$ is the mean gradient in the matrix area and $\mathbf{J}_{\text{inc}}$ is the mean gradient in the inclusions. The development below depends on how the interaction between the inclusions and the medium is described. For example, Maxwell's method was used by Zimmerman (1996) and Zimmerman et al. (1992) for calculating effective properties. However, this approach gives physically acceptable results only for a low-volume fraction p of inclusions or for the special case of nonoverlapping inclusions. Dagan (1989, p. 203, Figure 3.4.6 and Eq. 3.4.38) used a different approach by assuming that each inclusion is a composite spheroid with internal conductivity k_{inc} and external conductivity k_m, and that the ratio of internal to external volumes is p. This

composite spheroid is then placed in a medium with an effective conductivity value. Later, we will show that Dagan's approach does not produce as good a fit to the detailed numerical results as the approach used in this paper.

Now let us adopt Shvidler's approach (Shvidler, 1985) by assuming that all inclusions with intrinsic conductivity k_{inc} are placed in an effective medium. Next, to connect the gradient within inclusions and with the external gradient, we use the result of Landau and Lifshitz (1960) for polarization of the electric potential field by a single spheroid. Considering that each inclusion is placed within the medium with an effective hydraulic conductivity, the ratio between the projections of external gradient and the gradient projection within an inclusion can be written as:

$$J^{i}_{inc} = \xi_{ii} J^{i}_{ext} \tag{4a}$$

$$\xi_{ii} = \frac{k^{ii}_{ef}}{k^{ii}_{ef} - n_i\left(k^{ii}_{ef} - k_{inc}\right)} \tag{4b}$$

where k^{ii}_{ef} are the diagonal elements of effective hydraulic conductivity tensor $\mathbf{K}_{ef}$ and n_i are the polarization coefficients which depend on the shape of the spheroid.

For an oblate spheroid in 3D space, these coefficients have the following form (Shvidler, 1985):

$$n_3 = \frac{1+l^2}{l^3}\left[l - \tan^{-1}(l)\right]; \quad l = \sqrt{\varepsilon^2 \frac{k^{11}_{ef}}{k^{33}_{ef}} - 1} \tag{5a}$$

$$n_1 = n_2 = (1 - n_3)/2 \tag{5b}$$

For a 2D medium, the inclusions have the form of an ellipse and the polarization coefficients are:

$$n_1 = \frac{\varepsilon}{\varepsilon + \sqrt{\frac{k^{33}_{ef}}{k^{11}_{ef}}}} \quad n_3 = 1 - n_1 \tag{6}$$

The development below does not depend on the spatial dimension of the problem—that is, the results for 2D or 3D space differ only in the form of the polarization coefficients used). The spatial orientation of inclusions is taken into account by connecting the mean gradient projections, averaged over all inclusions, with the gradient projections for each inclusion given by Equation (4a).

2.2 A Regularly Oriented Set of Inclusions

Now consider several important cases of spatial inclusion orientation. For these, the main axes of all the inclusions are parallel to the axes of a global system of coordinates. Consecutively applying the external gradient along the x_1 axis—$J_{ext} = \{J^1_{ext}, 0, 0\}$—and along axis x_3—$J_{ext} = \{0, 0, J^3_{ext}\}$—we obtain from Equations (3a–b) and Equations (4a–b) the following system

of nonlinear equations for determining the main diagonal elements of effective hydraulic conductivity tensor:

$$k_{efv}^2(1-n_3)+k_{efv}\left[k_{inc}(n_3-p)+k_m(p+n_3-1)\right]-k_m k_{inc} n_3=0 \qquad (7a)$$

$$k_{efh}^2(1-n_1)+k_{efh}\left[k_{inc}(n_1-p)+k_m(p+n_1-1)\right]-k_m k_{inc} n_1=0 \qquad (7b)$$

where $k_{efh}=k_{ef}^{11}=k_{ef}^{22}$ is the horizontal effective hydraulic conductivity and $k_{efv}=k_{ef}^{33}$ is the vertical effective conductivity.

The system of Equations (7a) and (7b) is coupled via the polarization coefficients n_i, which depend on both components of the effective conductivity, according to Equations (5a–b) for the 3D case and Equation (6) for the 2D case. In general, the system of Equations (7a–7b) can only be solved numerically. For the simplest case of an isotropic medium (i.e., spherical inclusions), the values of the all polarization coefficients are equal to 1/3 and $k_{efh}=k_{efv}=k_{ef}$. Then, the effective conductivity value k_{ef} for this case can be found in a closed form shown by Equation (7a) (Odelevsky, 1951):

$$k_{ef}=\frac{k_{inc}}{4}\left\{(3p-1)+\nu(2-3p)+\sqrt{\left[(3p-1)+\nu(2-3p)\right]^2+8\nu}\right\} \quad \nu=\frac{k_m}{k_{inc}} \qquad (8)$$

2.3 A Randomly Oriented Set of Inclusions

In these cases, all inclusions are randomly oriented in space, and the directional cosines of inclusions are randomly distributed. Then, the effective hydraulic conductivity is characterized by one isotropic value k_{ef}. After applying an external gradient along the x_1 axis (i.e., $J_{ext}=\{J_{ext}^1,0,0\}$) and averaging over all inclusions, the projection of the mean gradient in an inclusion on x_1 (for 3D) has the form:

$$J_{inc}^1=\frac{\xi_{33}+2\xi_{11}}{3}J_{ext}^1 \qquad (9a)$$

For the 2D case, this equation is:

$$J_{inc}^1=\frac{\xi_{33}+\xi_{11}}{2}J_{ext}^1 \qquad (9b)$$

Together with Equations (3a–b), Equation (9a) yields the following expression for effective hydraulic conductivity:

$$k_{ef}=k_m+\frac{p}{3}(k_{inc}-k_m)(\xi_{33}+2\xi_{11}) \qquad (10)$$

Substitution of the coefficients ξ from Equation (4b) into Equation (10) yields an expression in closed form for p as the function of k_{ef} in 3-D space:

$$p=3\frac{(k_{ef}-k_m)\cdot\left[n_3(k_{ef}-k_{inc})-k_{ef}\right]\cdot\left[n_1(k_{ef}-k_{inc})-k_{ef}\right]}{k_{ef}(k_m-k_{inc})\cdot\left[k_{ef}(n_1+2n_3-3)-k_{inc}(n_1+2n_3)\right]} \qquad (11)$$

This equation allows the display relationship between k_{ef} and p in graphical form, calculating p values for given values of k_{ef}.

2.4 A Number of Inclusion Sets

The results obtained for one set of inclusions can be extended to the case of several sets of inclusions with different intrinsic hydraulic conductivities and anisotropies. Let us assume that N sets of inclusions, with volume fractions of each set p^i and the total volume fraction $\sum_{i=1}^{N} p^i < 1$, partially fill the medium with matrix conductivity. Applying the self-consistent equations for randomly oriented inclusions in 3-D space leads to the following formula:

$$k_{ef} = \frac{3k_m}{3 + \sum_{i=1}^{N} A^i p^i k_{inc}^i - k_m \sum_{i=1}^{N} A^i p^i} \tag{12a}$$

$$A^i = \frac{k_{ef}\left(n_i^i + 2n_3^i - 3\right) - k_{inc}^i\left(n_1^i + 2n_3^i\right)}{\left[n_3\left(k_{ef} - k_{inc}^i\right) - k_{ef}\right] \cdot \left[n_1\left(k_{ef} - k_{inc}^i\right) - k_{ef}\right]} \tag{12b}$$

where k_{inc}^i is the intrinsic hydraulic conductivity of i-th set and n_j^i is the polarization coefficient for i-th set of inclusions.

3 Verification against Theoretical and Numerical Results

In this section, we compare the effective hydraulic conductivity obtained by our self–consistent approach with analytical and numerical results found in the literature and with our own numerical modeling.

3.1 Verification against Theoretical Results

Theoretical results that predict the effective properties of a binary medium are limited. As examples, the equation of Dychne (1970) and some exact relations of percolation theory can be compared with our approach.

3.1.1 Analytical solution

Important theoretical results were obtained by Dychne (1970) for a 2D case. He showed that in a 2D binary isotropic system composed of geometrically equivalent subsystems, the following functional invariance relation (written in the notation of this paper) holds:

$$k_{ef}(p) \cdot k_{ef}(1-p) = k_m \cdot k_{inc} \tag{13a}$$

For the volume fraction of inclusion at 50%, this means:

$$k_{ef}\left(\frac{1}{2}\right) = \sqrt{k_m k_{inc}} \tag{13b}$$

Note that later, Zhikov et al. (1994) have shown that Equation (13a) is not rigorous for the arbitrary form of subsystems comprising the medium.

Using the polarization coefficients for isotropic inclusions in 2D space, $n_1 = n_3 = 1/2$, and solving Equation (7a) or Equation (7b), we obtain:

$$k_{ef} = (k_{inc} - k_m)(p - \frac{1}{2}) + \frac{1}{2}\sqrt{(1-2p)^2 (k_{inc} - k_m)^2 + 4k_{inc}k_m} \qquad (14)$$

which is consistent with Equation (13a).

The other rigorous result that can be used to test our approach is the effective conductivity of a horizontally layered medium. For such heterogeneity, the vertical effective conductivity is the harmonic mean and the horizontal effective conductivity is the arithmetic mean. For a horizontally layered medium $\lambda_h \to \infty$, $\varepsilon \to 0$ and $n_3 \to 1, n_1 \to 0$. Substituting this value $n_3 = 1$ into Equation (7a) and $n_1 = 0$ into Equation (7b), we see that these equations lead to the expected harmonic and arithmetic means.

3.1.2 Comparison with percolation theory

The self-consistent approach formally imposes no formal restrictions on the ratio of conductivities for the matrix and the inclusions, so that the effective conductivity can be calculated for the extreme case of an impermeable matrix. Putting $k_m = 0$ in Equations (8) and (14); we obtain the percolation threshold $p_c = 1/2$ for a 2D medium, and $p_c = 1/3$ for a 3D medium. The first value agrees with the precise percolation-theory result for a medium with hexagonal inclusions (Zhikov et al, 1994), but it is less than the experimentally obtained percolation threshold for circular inclusions of 0.669 (Lobb and Forster, 1987). The second value exceeds the theoretical percolation threshold for a 3D medium of 0.16 (Efros, 1988) by about a factor of two. The percolation exponent τ, i.e., the exponent of conductivity growth near the percolation threshold $k_{ef} \approx (p - p_c)^{\tau}$, equals 1.0 in both cases. This value matches well with the theoretical result for a 2D medium, but does not match well with the result for a 3D medium (τ=1.75) (Chiles and De Marsily, 1993). This comparison shows that our self-consistent approach produces a better result in a 2-D medium, at least for the case of an impermeable matrix.

3.2 Comparison with Numerical Modeling

3.2.1 3-D modeling result

Desbarats (1987) performed numerical modeling of flow in a 3D heterogeneous sand-shale formation with highly contrasting hydraulic conductivities of sand and shale. His purpose was to study the dependence of the effective hydraulic conductivity on: (1) the hydraulic conductivity contrast, (2) the volume fraction of shale, and (3) the anisotropy of the medium. Figure 2 shows the numerical results (Desbarats, 1987, Figure 12) for the case in which the ratio of hydraulic conductivities is equal to 10^4 and the coefficient of anisotropy ε is equal to 1/15. Also, in this

figure, the result of Dagan's approximation of effective hydraulic conductivity values (Dagan, 1989, fig 3.4.7 p. 205) is shown by dashed lines. The solid line is the calculated effective conductivity (horizontal and vertical) from the present approach, Equations (7a–b), by setting the matrix conductivity equal to the sand conductivity and the inclusion conductivity equal to the shale conductivity. This figure indicates that, in general, the agreement between numerical data and our results is good—better than the agreement between Dagan's results and numerical data.

3.2.2 2-D numerical modeling for estimation of effective hydraulic conductivity

In the aforementioned work of Debarats (1986), a relatively coarse grid (30 × 30 × 30) units and simple method (LSOR) were used for modeling of high-contrast conductivities. In our work, to eliminate the numerical effects and to more precisely model the 2D flow in a medium with inclusions, a 300 × 300 grid is used for the model domain. A randomly distributed set of inclusions oriented parallel to the main axes, with a coefficient of anisotropy $\varepsilon = 1/15$, is modeled within the domain. One inclusion covers 169 gridblocks. The volume fraction of inclusions p is changed within the range 0.05–0.95. Two values of hydraulic conductivity are used: the first is 1 m/d, which is the characteristic value for sand; the second is 10^{-4} m/d, which can be associated with shale conductivity.

For each modeling run with the set of inclusions given a p value, two conductivity fields are used. In the first (forward) case, the conductivity of inclusions equals the shale conductivity, and the matrix conductivity equals the sand conductivity. In the second (backward) case, conductivity assignments are switched. The conjugate gradient method with Cholethsky precondition is used to obtain accurate grid solutions for all values of p. The vertical and horizontal effective conductivity is calculated for each conductivity field (forward and backward) as functions of shale volume fraction p.

Figure 3 presents the numerical modeling results, together with results from calculating the effective conductivity using Equation (7a) and(7b). The figure shows that forward and backward curves for vertical and horizontal effective conductivities display hysteresis-like behavior. This hysteresis results from the different connectivity of fractions with high conductivity. In the forward curves, matrix conductivity is associated with sand, meaning that the sand bodies are almost perfectly connected, and this connection is destroyed only for high volume fraction of shale. In the backward curve, the matrix is associated with shale, and the sand bodies are inclusions, which means that the primary connection of the sand bodies is very poor. The ratio of forward to backward effective conductivities near the middle point (volume fraction of shale is 0.5) is about 5. Self-consistent curves shown in Figure 3 are very good fits with the forward curves within the range of shale volume 0–0.4 and with the backward curves within the range of shale volume 0.6–1.0. For shale volume 0.4–0.6, the self-consistent curves fall between the

forward and backward curves. That means that the self-consistent approach gives better results for the cases in which the connectivity of the highly conductive bodies does not play important role in the overall conductivity of the system. This is in keeping with the main thrust of our approach, that each inclusion interacts with the effective medium.

The evidence obtained from our simulations, of effective-conductivity hysteresis in the case of anisotropic inclusions, motivated us to perform additional simulations for isotropic inclusions, (i.e., for sets of circular inclusions for the p=0.5). According to Dychne (1970), the effective conductivity at this point is invariant (Equation (13b)), and its value for the used pair of sand and shale conductivities (1 and 0.0001) is 0.01. Five runs of numerical modeling for the forward and backward cases produced the results shown in Table 1. This table indicates that effective-conductivity hysteresis also exists for the isotropic case, in which the ratio of forward and backward values is about two orders of magnitude. Note however, that the geometric mean of forward and backward values for this case agrees very well with the Dychne theory and the self-consistent results.

Table 1. Results of modeling flow in sand/shale formation for shale volume fraction 0.5.

Run	k_{ef} forward - k_{ef}^{f}	k_{ef} backward - k_{ef}^{b}	$\sqrt{k_{ef}^{f} k_{ef}^{b}}$	k_{ef}^{f} / k_{ef}^{b}
1	0.136	0.00059	0.0090	230
2	0.0938	0.00110	0.0102	84
3	0.1358	0.00115	0.0125	117
4	0.1126	0.00079	0.0094	142
5	0.0989	0.00084	0.0091	116
Mean	0.115	0.0009	0.010	127

These results once more show the importance of connectivity among the highly permeable bodies on the overall effective conductivity of the medium.

4 Effective Conductivity of a Fractured Porous Medium

In recent decades, the hydraulic conductivity of fractured and fractured porous media has been the subject of intensive theoretical studies. These investigations began with the work of Romm (1966) and Snow (1969), who produced the first results for a system of infinite fractures in 2D and 3D space. Later, finite fracture sizes and low fracture density (with their effect on fracture connectivity) were considered by Robinson (1983), Long and Witherspoon (1985) and others. More recent developments deal with stochastic simulation of fracture networks in 3D and investigations of how fracture statistical parameters influence overall hydraulic conductivity

(Chiles and De Marsily, 1993, Bour and Davy, 1998). Extensive studies were performed to analyze flow in single-plane fractures with variable aperture (Tsang, 1993; Gelhar, 1993; Zimmerman and Yeo, 2000) and to understand the effect of the contact area on the permeability of fractures (Zimmerman et al., 1992).

The self-consistent approach can be effectively used for calculating flow in fractured and fractured porous media, owing to the principal features of these rocks:

1. Fractures that have intrinsic conductivity k_f can be considered as inclusions into the matrix medium with much lower (down to zero) conductivity k_m.
2. The total volumetric fraction of inclusions (i.e., fracture porosity) is quite small: p<<1.

In this section, we report some results obtained by our approach for fractured and fractured porous media.

4.1 Flow in Single-Plane Fractures with Contact Areas

Zimmerman, Chen, and Cook (1992) studied flow in a single fracture with contact areas, using the Maxwell approach for circular and elliptical shaped contact areas. They considered 2D flow in fractures using the "cubic law"; i.e., setting fracture transmissivity to be proportional to the aperture cubed and equal to zero in the contact area. In this case, the effective fracture transmissivity, or effective hydraulic aperture, continuously changes with the changing of the contact areas p from 0 to 1, without a percolation threshold. According to Equation (14), an applying the self-consistent approach for the case with circular contact areas of zero fracture transmissivity produces the following results:

$$T_{ef} = T_f (1 - 2p) \qquad (15)$$

where T_{ef} is the effective transmissivity of fracture, $T_f = b \cdot k_f = \frac{1}{12} b^3$ is the transmissivity of the fracture outside the contact areas, b is the fracture aperture outside the contact areas, and p is the fraction of contact area over the fracture plane. Equation (15) yields zero transmissivity when p is more than 0.5.

Table 1 shows the results of a 2D simulation of a highly conductive medium, with circular inclusions that have hydraulic conductivity four orders of magnitude less than the conductivity of the medium. This result shows that for p=0.5 the effective hydraulic conductivity is not zero, but it is about 0.11 of the medium's conductivity. This is a function of the connectivity of a highly conductive medium, parts of which are still not isolated by inclusions. Taking this finding into account, we postulate that the equation for effective fracture transmissivity in this type of medium can be written in the following form:

$$T_{ef} = T_f\left(1 - 2p + a_2 p^2 + ...\right) \quad (16a).$$

Correspondingly, the second-order approximation for the effective hydraulic aperture of fractures with contact areas is:

$$b_{ef} = b \cdot \sqrt[3]{\frac{1 - 2p + a_2 p^2}{1 - p}} \quad (16b).$$

Substitution of the numerical result for the ratio T_{ef}/T_f of 0.11 at p = 0.5 gives the value for $a_2 \approx 0.44$ and the corresponding percolation threshold at $p_{cr} \approx 0.57$. Note that this value for p_{cr} is less than that obtained by Lobb and Forster (1987), who calculated the percolation threshold for circular inclusions to be 0.669, probably because inclusions are not perfectly circular with a square numerical grid—and for a 2D system, percolation threshold depends on the shape of the inclusions (Zhikov et al, 1994). Using data from Lobb and Forster (1987) (see Zimmerman, 1996, Figure 6) we found that if we set a_2=0.78, Equation 16a is good for predicting conductivity with circular contact areas up to the percolation threshold.

4.2 Flow in a Parallel System of Finite-Sized Fractures

It is well known that the effective hydraulic conductivity of a fractured porous medium with low permeable matrix and disconnected fractures can be one or two orders magnitude greater than the matrix conductivity. The theories of Romm (1966) and Snow (1969) cannot help in predicting the effective conductivity of such a system, because of the finite fracture size and fracture disconnectedness. In this section, we derive the equations for calculating the effective hydraulic conductivity of such a system and verify them for 2-D and 3-D cases against other solutions.

4.2.1 Regular fracture network in two-dimensional space

Malkovsky and Pek (1995) numerically studied the effective hydraulic conductivity of a 2D fractured porous medium with a regular fracture network geometry (shown in Figure 4. They developed an analytical approximation for the effective hydraulic conductivity along the fracture direction, of the following form:

$$k_{ef}^{11} = k_m\left(1 + \frac{A(M)}{\left[h^{B(M)} + 0.125\sqrt[4]{h}(l-1)^5\right]\sqrt[4]{l-1}}\right) \quad (17a)$$

$$A(M) = 2.143\left(1 - e^{-0.487M}\right); \quad B = 0.9687 + 0.8138\left(1 - e^{-0.09261M}\right) \quad (17b)$$

$$h = \frac{H}{L_1}, \; l = \frac{L}{L_1}, \; M = \frac{\delta \cdot k_f}{L_1 k_m} \quad (17c)$$

where $2L_1$ is the fracture length, 2δ is the fracture aperture, $2L$ is the distance between fracture centers in one row, B is the distance between neighboring fracture rows, k_f is the fracture hydraulic conductivity, and k_m is the matrix hydraulic conductivity.

For this geometry, the fracture porosity p is equals to $L_1\delta/(2LH)$. Then, Equations (17a) and (17b) are valid within the following range of parameters:

$1.25<l<2$, $0.1<h<5$, $0.2<M<500$. (17d)

To apply the self-consistent approach to this problem, we represent a rectangular fracture by an equivalent elliptical fracture with an anisotropy aspect ratio equal to the ratio of rectangular fracture aperture to fracture length: $\varepsilon = \delta / L_1$ and with the same area (Figure 4c). For this system, the effective hydraulic conductivity in the direction orthogonal to the direction of fractures is approximately the same as the matrix conductivity, $k_{ef}^{33} \approx k_m$. Thus, the effective hydraulic conductivity along the fracture direction can be found from the following equation for self-consistent conductivity:

$$\left(k_f - k_m\right)\frac{k_{ef}^{11}}{k_{ef} - n_1\left(k_{ef}^{11} - k_m\right)}p + k_m - k_{ef}^{11} = 0 \qquad (18)$$

where the polarization coefficient n_1 is calculated, taking into account that $k_{ef}^{33} \approx k_m$:

$$n_1 = \frac{\varepsilon}{\varepsilon + \sqrt{\frac{k_m}{k_{ef}^{11}}}} \qquad (19)$$

This leads to the following polynomial equation for computing the effective hydraulic conductivity along the fracture direction:

$$-\bar{k}_{ef} + \varepsilon\left[\bar{k}_f\left(p-1\right) - p\right]\sqrt{\bar{k}_{ef}} + \frac{\varepsilon\,\bar{k}_f}{\sqrt{\bar{k}_{ef}}} + 1 + p\left(\bar{k}_f - 1\right) = 0 \qquad (20)$$

where $\bar{k}_{ef} = k_{ef}^{11} / k_m$, $\bar{k}_f = k_f / k_m$.

For the special case of highly conductive fractures, when $\varepsilon\bar{k}_f \to \infty$, the solution of Equation (20) can be written in explicit form as:

$$\bar{k}_{ef} = 1 + \frac{1}{2}I \cdot \left(I + \sqrt{I^2 + 4}\right) \qquad (21a)$$

$$I = p / \varepsilon = 4N_2L_1^2 \qquad (21b)$$

where N_2 is the spatial density of fracture centers in 2-D space.

Comparison of the numerical solution Equation (20) and Equation (21a) shows that Equation (21a) is valid for the cases when $\varepsilon\bar{k}_f \geq 20$.

To compare the results obtained by Malkovsky and Pek (1995) with the above equations for the self-consistent hydraulic conductivity, we computed 3,000 values of effective hydraulic conductivities, using both approaches for fracture parameters randomly distributed within the ranges given in Equation (17d).

The results of this comparison are shown in Figure 5. This figure indicates that the self-consistent approach produces a good agreement with the Malkovsky and Pek (1995) results for the effective hydraulic conductivity of a regular parallel set of fractures. The advantages of using the self-consistent approach for such a system are that it is not under any formal limitations on fracturing parameters like Equation (17d), and Equation (20) can be used for any parallel systems of fractures.

4.2.2 Parallel fracture network in three-dimensional space

A approach similar to that for the 2D system is applicable for disk fractures in 3D that are parallel to one axis. The same precondition is used—that the effective hydraulic conductivity in the direction orthogonal to the fracture plane is equal to the matrix conductivity $\left(k_{ef}^{33} \approx k_m\right)$. Then, a good 3D approximation for the polarization coefficient n_1 has the following form:

$$\frac{1}{n_1} = a_0 + \frac{a_1}{\varepsilon^0}, \quad \varepsilon^0 = \varepsilon\sqrt{k_{ef}^{11}/k_{ef}^{33}}, \quad a_0 = 1.621, a_1 = 1.273 \tag{22}$$

This equation is valid with error less than 1% for $\varepsilon^0 < 0.2$. Substitution of Equation (22) into Equation (18) leads to a polynomial equation for calculating the effective hydraulic conductivity in three-dimensional space:

$$\begin{aligned} &a\bar{k}_{ef}^2 + b\bar{k}_{ef}^{\frac{3}{2}} + c\bar{k}_{ef} + d\sqrt{\bar{k}_{ef}} + \varepsilon\bar{k}_f = 0 \\ &a = \varepsilon(1-a_0), b = -a_1, c = \varepsilon\left\{a_0\left[p\left(\bar{k}_f - 1\right)+1\right]-1-\bar{k}_f\right\}, d = a_1\left[1+p\left(\bar{k}_f - 1\right)\right] \end{aligned} \tag{23}$$

For the case of highly conductive fractures, when $\varepsilon\bar{k}_f \to \infty$, the solution for effective conductivity can be written in an explicit form:

$$\bar{k}_{ef} = 1 + \frac{1}{2} Ia_1\left(Ia_1 + \sqrt{I^2a_1^2 + 4}\right) \tag{24a}$$

$$I = p/\varepsilon = \frac{\pi}{6} N_3 D^3 \tag{24b}$$

where N_3 is the density of fracture centers in 3-D space, D is the fracture disk diameter. Equation (24a) is valid with errors less 10% , for $\varepsilon\bar{k}_f \geq 100$ and for the fracture porosity p less than 0.01.

To verify the effective hydraulic conductivity values in 3-D obtained as the roots of Equation (23), we performed a numerical calculation of flow in a fractured porous medium. We modeled a 3D steady-state flow between two opposing vertical faces of a block having a set of horizontal, parallel, disk-shape fractures randomly distributed in it space. The grid had dimensions 100 × 100 × 40, with a constant gridblock side of 0.1 m in all dimensions. Each fracture disk has a diameter of 0.9 m and an aperture of 10^{-4} m. The ratio of fracture-matrix conductivities is 10^5. First, for each modeling run, a set of randomly distributed fractures was simulated. Next, the

matrix hydraulic conductivity value was assigned to be the vertical hydraulic conductivity value for each gridblock. The horizontal hydraulic conductivity value for each block was calculated as:

$$k_b^h = p_i k_f + (1 - p_i) k_m,\ p_i = \frac{N_i 2\delta}{\Delta z} \qquad (25),$$

where k_b^h is horizontal block hydraulic conductivity, 2δ is fracture aperture, Δz is the side length of the block, and N_i is the number of fractures within i-th block.

Figure 6 shows the results of numerical simulation and the calculated effective hydraulic conductivity from Equation (23). Two different curves for effective conductivity are obtained, using different ways of representing the disk fracture with constant aperture and using an ellipsoid that has the same volume. The first curve is calculated using the same value of the ellipsoid anisotropy aspect ratio as the ratio of fracture aperture to fracture diameter. The second curve is calculated with the precondition that the ellipsoid diameter is equal to fracture diameter. In this latter case, the ellipsoid anisotropy aspect ratio equals 3/2 of the ratio of fracture aperture to fracture diameter. Figure 6 indicates that numerical results are well fitted by self-consistent values, and they generally fall between these two alternative self-consistent curves over the typical range of fracture porosity.

4.3 Randomly Oriented System of Fractures

4.3.1 Random fracture set in two dimensional space

Consider a two-dimensional fracture set consisting of randomly oriented fractures of constant length L. The effective hydraulic conductivity of this system is isotropic and characterized by a single value k_{ef} in all directions. Combining Equations (3a–b), Equation (6), and Equation (9b) produces the following polynomial expression of the third order for effective hydraulic conductivity:

$$-\varepsilon \cdot k_{ef}^3 + b \cdot k_{ef}^2 + c \cdot k_{ef} + \varepsilon \cdot k_m k_f^2 = 0 \qquad (26)$$

where : $b = k_m\left(-\frac{p}{2}\left(1+\varepsilon^2\right)+\varepsilon(1-p)\right)+k_f\left(\frac{p}{2}\left(1+\varepsilon^2\right)+\varepsilon(p-\varepsilon)-1\right)$, and

$$c = -k_f \cdot k_m\left(\frac{p}{2}\left(1+\varepsilon^2\right)+\varepsilon(p-\varepsilon)-1\right)+k_f^2\left(\frac{p}{2}\left(1+\varepsilon^2\right)+\varepsilon(p-1)\right).$$

For infinite fractures $(\varepsilon \to \infty)$ the solution of Equation (26) is:

$$k_{ef} = k_f \frac{k_f p + k_m(2-p)}{k_f(2-p) + k_m p} \qquad (27a).$$

For the typical case of fractured medium, i.e., $p<<1$ and $k_m<<k_f$, Equation (27a) tends to:

$$k_{ef} \approx k_m + k_f \frac{p}{2} \qquad (27b)$$

This equation for impermeable matrix reproduces the result of Romm (1966) and Snow (1969) for a 2D random fracture network.

Equation (26) yields the effective hydraulic conductivity for arbitrary values of parameters. The most critical task of the self-consistent approach is predicting the hydraulic conductivity of a purely fractured medium near to percolation threshold. Consider the effective permeability of a low-density fractured medium for the case of $k_m = 0$. The relationship between the fracture porosity p and the geometric characteristics of elliptical fractures, with fracture density N_2 and fracture length L, can be written in the form:

$$p = \varepsilon \frac{\pi}{4} N_2 L^2 \qquad (28a)$$

Substitution of the porosity from Equation (28a) into Equation (26) and setting the effective conductivity equal to zero produces the following critical dimensionless fracture density at the percolation threshold:

$$N_2 L^2 = \frac{8}{\pi\left(1 + 2\varepsilon + \varepsilon^2\right)} \qquad (28b)$$

This equation gives the numerical value for percolation threshold as 2.54, which is about two times less of the value (5.7) obtained for a random network based on intensive numerical simulation conducted by different authors (Robinson, 1983; Bour, Davy, 1998). Solving Equation (26), the growth of the effective hydraulic conductivity near the percolation threshold for very thin fractures $(\varepsilon \to \infty)$ is described by:

$$\frac{k_{ef}}{k_\infty} = 1 - \frac{8}{\pi \cdot N_2 L^2} \qquad (28c)$$

where $k_\infty = k_f\, p/(2 - p)$ is the effective conductivity of infinite fractures network (see Equation 27a).

Equation (28c) differs from the equation for effective conductivity of a sparsely fractured medium proposed by Robinson (1984). Figure 7 reproduces Figure 4.54 (p.192) of Gelhar (1993), in which numerical results of different authors were compared with the Robinson (1984) equation. The line representing Equation (28c) is also shown in this figure. We can see that, despite the fact that Equation (28c) generates more rapid growth in effective conductivity, generally the results found for the 2-D network using the self-consistent approach appear to be physically acceptable. Note also that numerical results are well bracketed between Robinson's curve and the self-consistent curve (Figure 7)

4.3.2 A random fracture set in three-dimensional space

The development of the two-dimensional fracture set presented in the previous section is applicable to the much more realistic case of fracturing represented by 3D random-orientation fractures of constant diameter D. For the 3D case, a third-order polynomial equation for calculation of effective hydraulic conductivity is also obtained:

$$a \cdot k_{ef}^3 + b \cdot k_{ef}^2 + c \cdot k_{ef} - k_m k_f^2 n_1 (1 - 2n_1) = 0 \qquad (29)$$

where $a = 2n_1(1 - n_1)$; $b = k_f\left(1 - 3n_1 - \frac{p}{3} - pn_1 + 4n_1^2\right) + k_m\left(\frac{p}{3} - 2n_1 + 2n_1^2 + pn_1\right)$

$c = k_f^2\left(n_1 + pn_1 - \frac{2p}{3} - 2n_1^2\right) + k_f k_m\left(3n_1 - 4n_1^2 + \frac{2}{3}p - pn_1 - 1\right)$.

For infinite fractures $(n_1 \to 0)$, the solution of Equation (29) is

$$k_{ef} = k_f \frac{2p(k_f - k_m) + 3k_m}{3k_f - p(k_f - k_m)} \qquad (30a)$$

For the typical case of a fractured medium (i.e., p<<1 and k_m<<k_f), Equation (30a) tends to:

$$k_{ef} \approx k_m + k_f \frac{2p}{3} \qquad (30b)$$

Consider the effective permeability of a low-density fractured three-dimensional medium for the case $k_m = 0$. The relationship between the fracture porosity p, the geometric characteristics of ellipsoidal fractures with fracture density N_3, and fracture diameter D has the form:

$$p = \varepsilon \frac{\pi}{6} N_3 D^3 \qquad (31a)$$

Substituting porosity from Equation (31a) into Equation (29), taking into account the approximation of Equation (22) for the polarization coefficient n_i, and setting the effective conductivity to zero—gives the following critical dimensionless fracture density at the percolation threshold:

$$N_3 D^3 = \frac{9}{\pi \cdot a_1} \approx 2.25 \qquad (31b)$$

This value falls within the range of values for the percolation threshold given by Chiles and De Marsily (1993), but generally exceeds the upper limit for percolation threshold given by most other authors. For example, Gelhar (1993), referring to different works, places the interval for critical fracturing density between 1 and 2.

The growth of the effective hydraulic conductivity near the percolation threshold for very thin fractures $(\varepsilon \to \infty)$ is described by:

$$\frac{k_{ef}}{k_\infty} = 1 - \frac{9}{\pi \cdot a_1 \cdot N_3 D^3} \qquad (31c)$$

where $k_\infty = k_f 2p/(3-p)$ is the effective conductivity of an infinite fractures network (see Equation 30a).

5 Conclusion

In this paper, a self-consistent approach has been applied to calculate the effective hydraulic conductivity of a heterogeneous medium composed of highly contrasting intrinsic permeability values. This approach does not have formal limitations on the difference in intrinsic permeability values between the two materials. Thus, formally, it can be used for the case in which one material is impermeable.

The effective parameters obtained by this approach generally agree with numerical 2-D and 3-D modeling results, done for the case of four-orders-of-magnitude contrast between the intrinsic permeabilities of the materials.

Verification of this approach against the percolation theory shows that this approach gives physically acceptable results for the case of isometric permeable inclusions placed into impermeable medium. Our 2D results for the percolation threshold agree with the percolation theory, while our results for a 3D medium exceed the percolation threshold by almost a factor of two. For the cases of highly anisotropic inclusions (i.e. fractures in 2D and 3D) in an impermeable matrix, the percolation thresholds and the growth of effective conductivity are obtained. The results are close to those of the percolation theory, although specific values of relative fracture density do not exactly match.

The main limitations of the present approach have to do with its invariance to assigned medium/inclusion intrinsic permeability values. Our modeling results show that, near the middle point of the inclusion volume fractions, the effective conductivity strongly depends not only on the ratio of conductivities in the medium/inclusion and the inclusion geometry, but also on what value is assigned to the medium and the inclusions. For highly conductive media and weakly conductive inclusions, the effective hydraulic conductivity could be up to one order of magnitude larger than the conductivity for the complementary case. The self-consistent approach gives a value near the geometric average of both cases. This limitation is associated with the nature of our approach, in that inclusions interact with effective media and not directly with each other, whereas the observed behavior of the effective conductivity are often a result of the interaction of highly conductive bodies with each other.

As a practical application, the present approach can be effectively used for the cases of spatially distributed hydraulic conductivity in sand-shale and fractured porous aquifers, based on geostatistical simulation of heterogeneity. This can be done using measurable heterogeneity

parameters (such as fracture density and sand volume fraction) and constructing model blocks with spatially distributed parameters. Then, the self-consistent conductivity can be calculated for these blocks using equations from this paper.

Acknowledgement

This work was accomplished with support from the Civilian and Development Research Foundation (CRDF) through Contract No. RG2-2395-MO-02. Also, the first author would like to express his appreciation to the CRDF Grant Assistance Program and the Ernest Orlando Lawrence Berkeley National Laboratory (LBNL) for supporting his visit to LBNL to conduct research described in this paper through Contact 6510723/RG0-1254. The second authors would like to acknowledge the support of the Geosciences and Engineering Office, Office of Science, Office of Basic Energy Science, of the U.S. Department of Energy under Contract No. DE-AC03-76SF00098.

References

Bour, O., and P. Davy, On the connectivity of three-dimensional fault networks, *Water Resources Res.*, 34(10), 2611–2622, 1998

Chiles J.P., and G. De Marsily, Stochastic models of fracture systems and their use in flow and transport modeling, in *Flow and Contaminant Transport in Fractured Rock*, edited by Bear J., Chin-Fu Tsang, and G. Marsily, 169–235, 1993.

Dagan, G., *Flow and Transport in Porous Formations*, Springer-Verlag, New York, 1989.

Dagan, G., and S.C. Lessoff, Solute transport in heterogeneous formations of bimodal conductivity distribution, *Water Resources Res.* 37(3), 465–642. 2001.

Desbarats, A. J., Numerical estimation of effective hydraulic conductivity in sand-shale formations, *Water Resources Res*. 23(2), 273–286, 1987.

Dychne, A.M., Transmissivity of 2-D two phases system, *Journal Experimental and Theoretical Physics*, 59(1) 111-115, 1970 (in Russian).

Efros, A.L., *Physics and Geometry of Chaos*, Kvant, Moscow. 1988 (in Russian).

Fogg, G. E., Groundwater Flow and Sand Body Interconnectedness in a Thick Multiple-Aquifer System, *Water Resources Res. 22* (5), 679–694, 1986.

Gelhar L.W., *Stochastic subsurface hydrology*, Prentice Hall Englewood Cliffs, New Jersey 07635, 1993.

Landau, L.D., and E.M. Lifshitz, *Electrodynamics of Continuous Media*, Pergamon, New York, 1960.

Lobb, C. J., and M.G. Forrester, Measurement of nonuniversal critical behavior in a two dimensional percolating system. *Phys. Rew*. B35, 1899–1901. 1987.

Long, J.C.S., and P.A. Witherspoon, The relationship of degree of interconnection to permeability in fracture networks, *J. Geophys. Res*., 90 (B4), 3087–3098, 1985.

Malkovsky, V.I., and A.A. Pek, Evaluation of the permeability of fractured-porous medium with a regular system of discrete parallel fractures, *Petrology* 3 (2), 223–224, 1995.

Odelevsky, V.I., Calculation of effective conductivity of heterogeneous system, *Journal Technical Physics*, XXI (6), 667-685. 1951 (in Russian).

Oda, M., An equivalent continuum model for coupled stress and fluid flow analysis in jointed rock masses, *Water Resources Res*., 22(12), 1845-1856, 1986.

Robinson, P.C., Connectivity of fracture system—A percolation theory approach, *J. Phys. A: Math. Gen.*, 16, 605–614, 1983.

Romm, E.S., *Hydraulic properties of fractured rocks*. Nedra, Moscow, 1966 (in Russian).

Rouleau, A., and J.E. Gale, Stochastic discrete fracture simulation of groundwater flow into an underground excavation in granite, *Int. J. Rock mech. Min. Sci. and geomech. Abstr*., 24(2), 99–112, 1987.

Rubin, Y., Flow and transport in bimodal heterogeneous formations, *Water Resources Res*., 31(10), 2461–2468, 1995.

Snow, D.T., Anisotropic Hydraulic conductivity of Fractured Media, Water Resources Res., 5(6), 1273–1289, 1969.

Shvidler, M.I., *Stochastic Hydrodynamics of Porous Medium*, Nedra, Moscow, 1985 (in Russian).

Tsang, C.-F., Tracer transport in fracture systems, in *Flow and Contaminant Transport in Fractured Rock*, edited by Bear J., C.-F. Tsang, and G. Marsily, 237–266, 1993.

Zimmerman, R.W., Effective conductivity of two-dimensional medium containing elliptical inhomogeneities, *Proc. R. Soc. Lond.* A. 452, 1713–1727, 1996.

Zimmerman, R.W., and I.-W. Yeo, Fluid flow in rock fractures: From the Navier-Stokes Equation to the Cubic Law, in *Dynamics of Fluids in Fractured Rock*, edited by B. Faybishenko, P.A. Witherspoon and S.M. Benson, AGU Geophysical Monograph 122, 213–224, 2000.

Zimmerman, R.W., D.W. Chen, and N.G.W. Cook, The effect of contact area on the permeability of fractures, *J. Hydrology*, 139, 79–96, 1992.

Zhikov, V.V., S.M. Kozlov, and O.A.Oleinik., *Homogenization of Differential Operators and Integral Functionals*, Springer-Verlag, Berlin, 1994.

Figure captions

Figure 1. Representation of medium hydraulic heterogeneity by matrix and inclusions

Figure 2. The comparison of self-consistent results found by solving system of Equations 7a and 7b for 3D flow with numerical results of Desbarats (1987) and Dagan's approximation. Symbols are numerical results for anisotropy coefficient 1/15, solid lines are self-consistent curves for vertical and horizontal effective conductivity, and the dotted lines are Dagan's approximation of conductivities.

Figure 3. The comparison of self-consistent results found by solving system of Equations 7a and 7b for 2D flow with numerical modeling. Lines with symbols are numerical results for anisotropy coefficient 1/15. The forward runs are shown by open symbols and backward runs are shown by filled symbols. Thick lines are self-consistent curves for the vertical and horizontal effective conductivity

Figure 4. Geometry of a 2D regular fracture network problem in a medium with matrix conductivity studied by Malkovsky and Pek (1995): (a) view of fracture network, (b) geometry of periodic fracture cell G and (c) representation of rectangular fracture by equivalent elliptical fracture.

Figure 5. Comparison of self-consistent hydraulic conductivity calculated using Equation (20) with the values of effective hydraulic conductivity, calculated using the Malkovsky and Pek (1995) equation.

Figure 6. Effective hydraulic conductivity of a 3D matrix medium with a set of parallel disk fractures randomly distributed over space. Filled circles were obtained by numerical simulation and the curves are the self-consistent hydraulic conductivity calculated as the root of the polynomial expression (Equation (23)). The curves are labeled by the values of the ellipsoidal fracture anisotropy aspect ratio used.

Figure 7. Comparison of the effective hydraulic conductivity near the percolation threshold obtained by the self-consistent approach (solid line) with that given by Robinson (1984) equation (dash line) and results from numerical simulations.

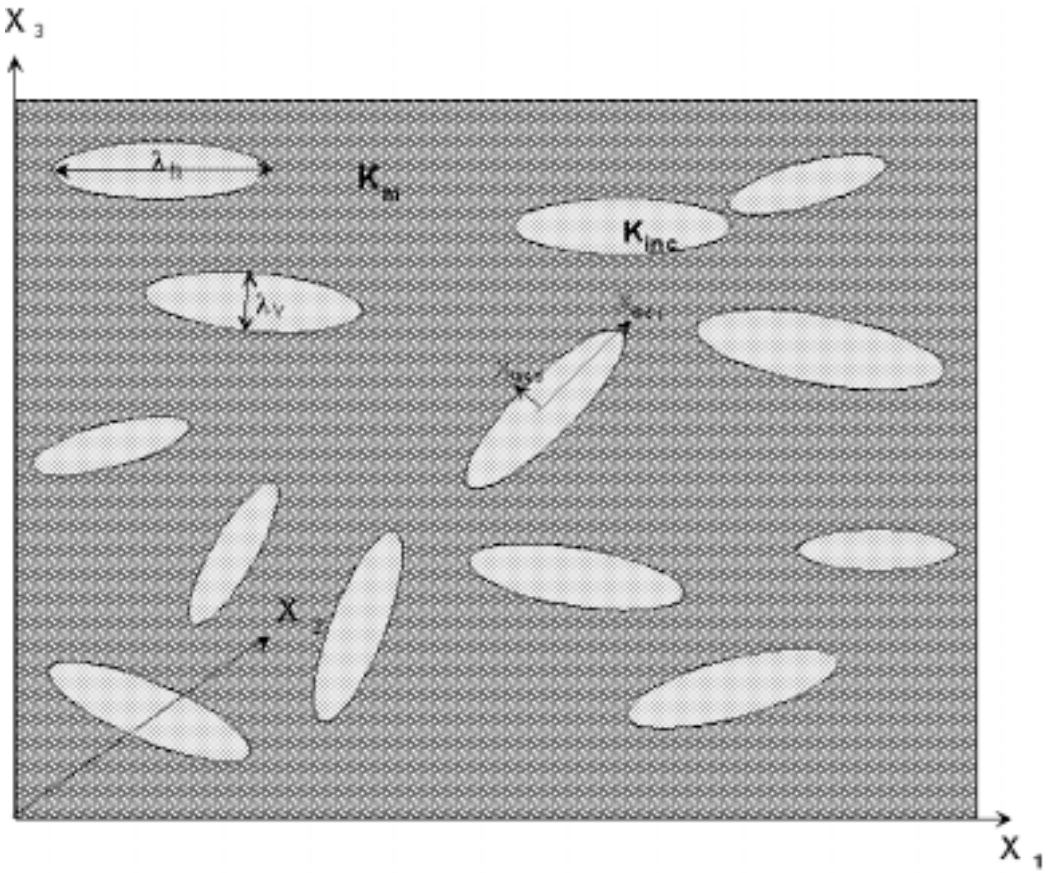

Figure 1.

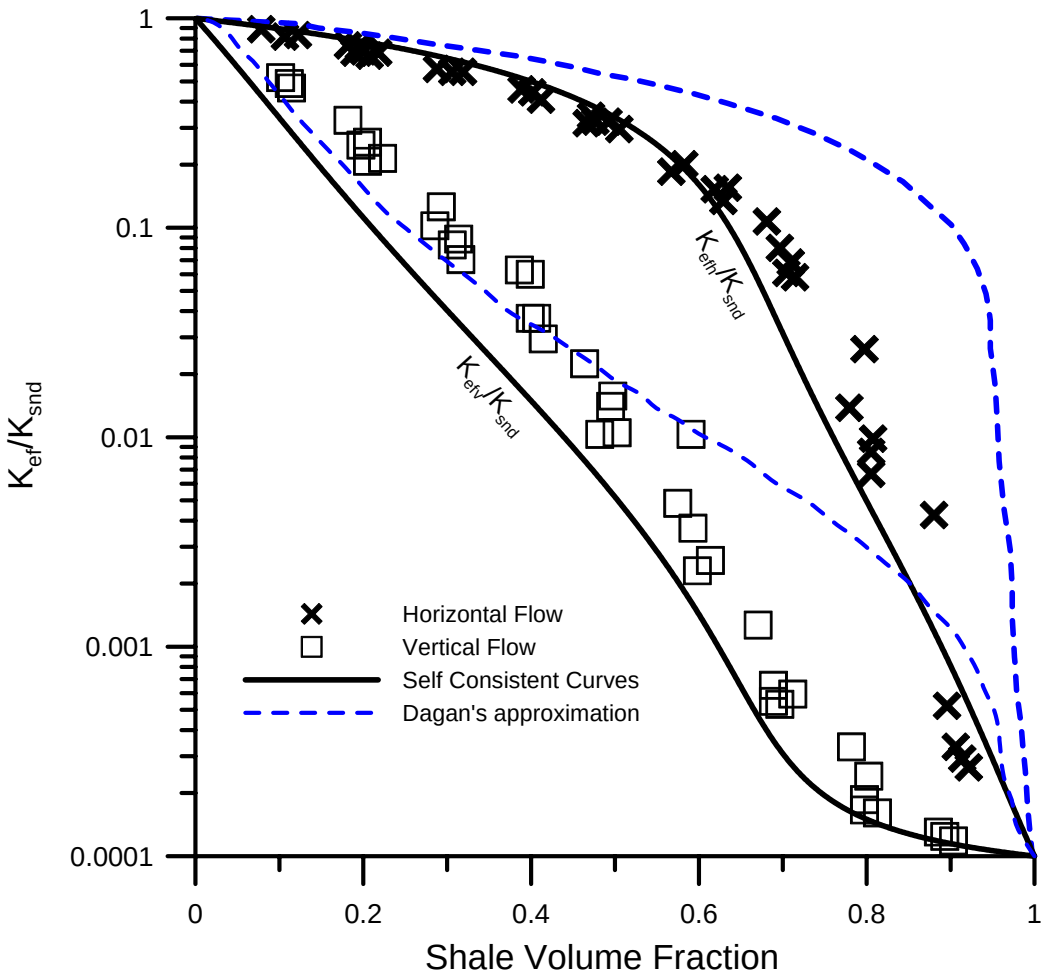
1
0.1
0.01
0.001
0.0001
0
0.2
0.4
0.6
0.8
1
Shale Volume Fraction
K_ef/K_snd
K_efh/K_snd
K_efv/K_snd
Horizontal Flow
Vertical Flow
Self Consistent Curves
Dagan's approximation

Figure 2.

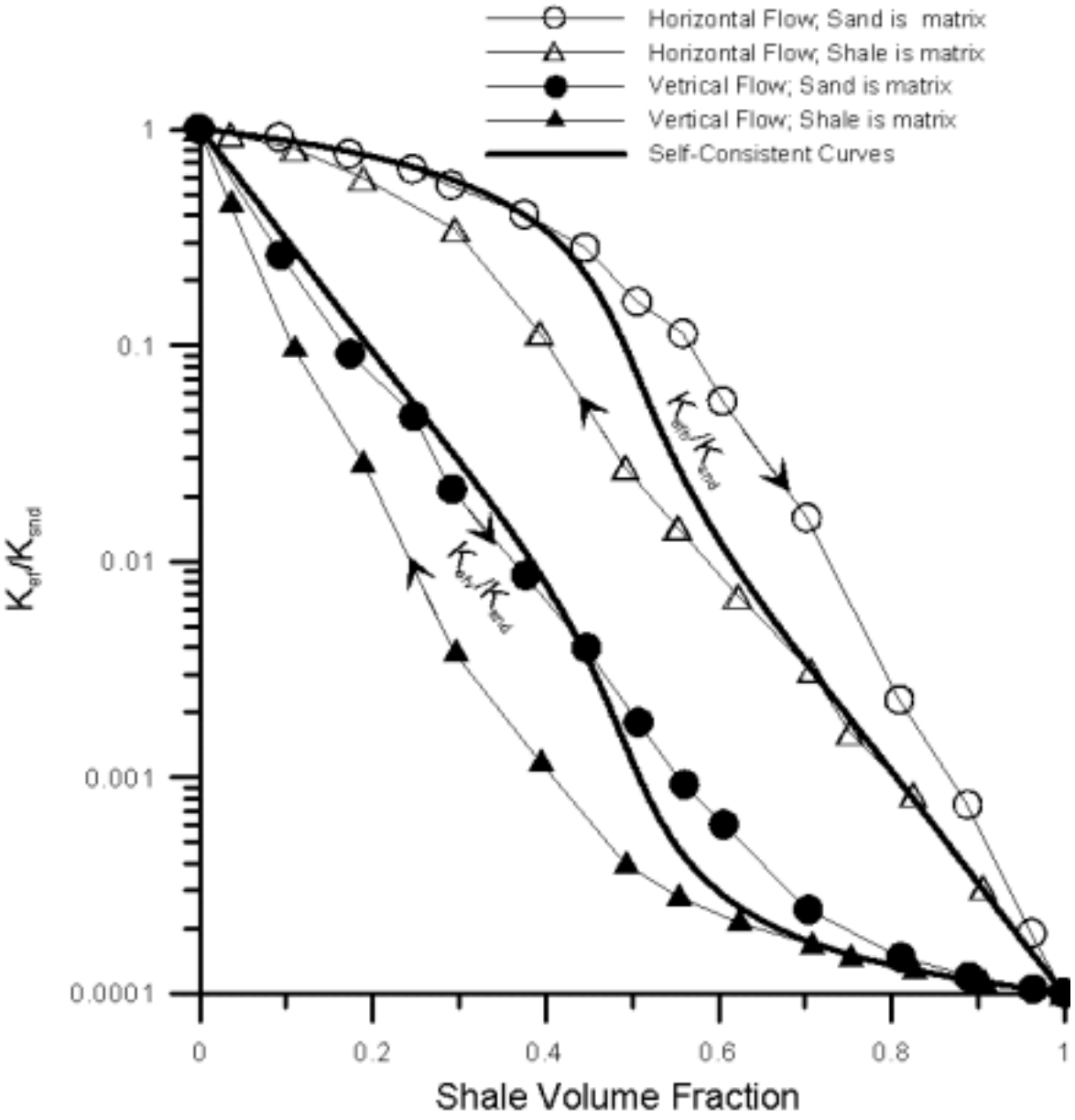
Horizontal Flow; Sand is matrix
Horizontal Flow; Shale is matrix
Vetrical Flow; Sand is matrix
Vertical Flow; Shale is matrix
Self-Consistent Curves
1
0.1
0.01
0.001
0.0001
0
0.2
0.4
0.6
0.8
1
Shale Volume Fraction
K_eff/K_snd
K_eff/K_snd

Figure 3.

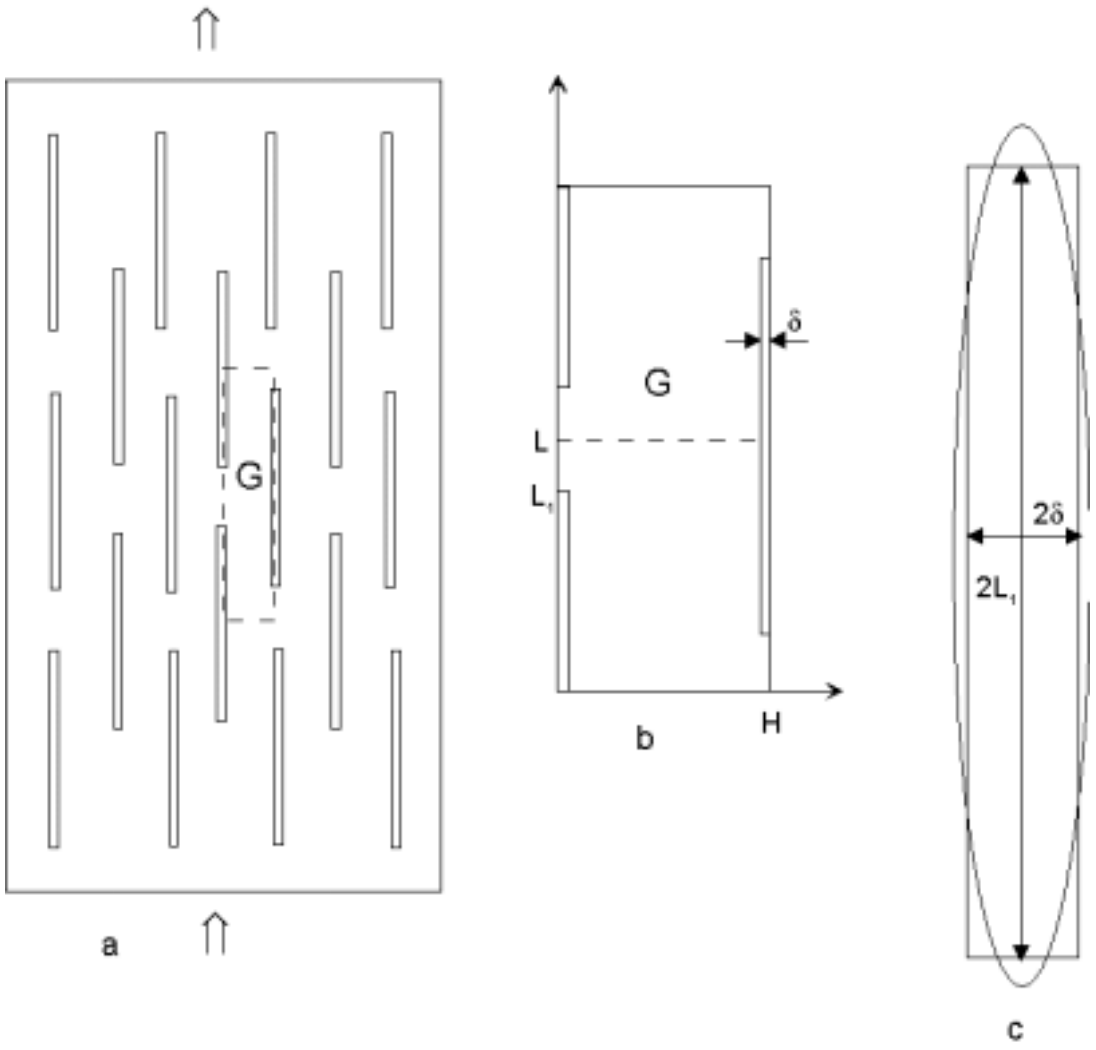

Figure 4.

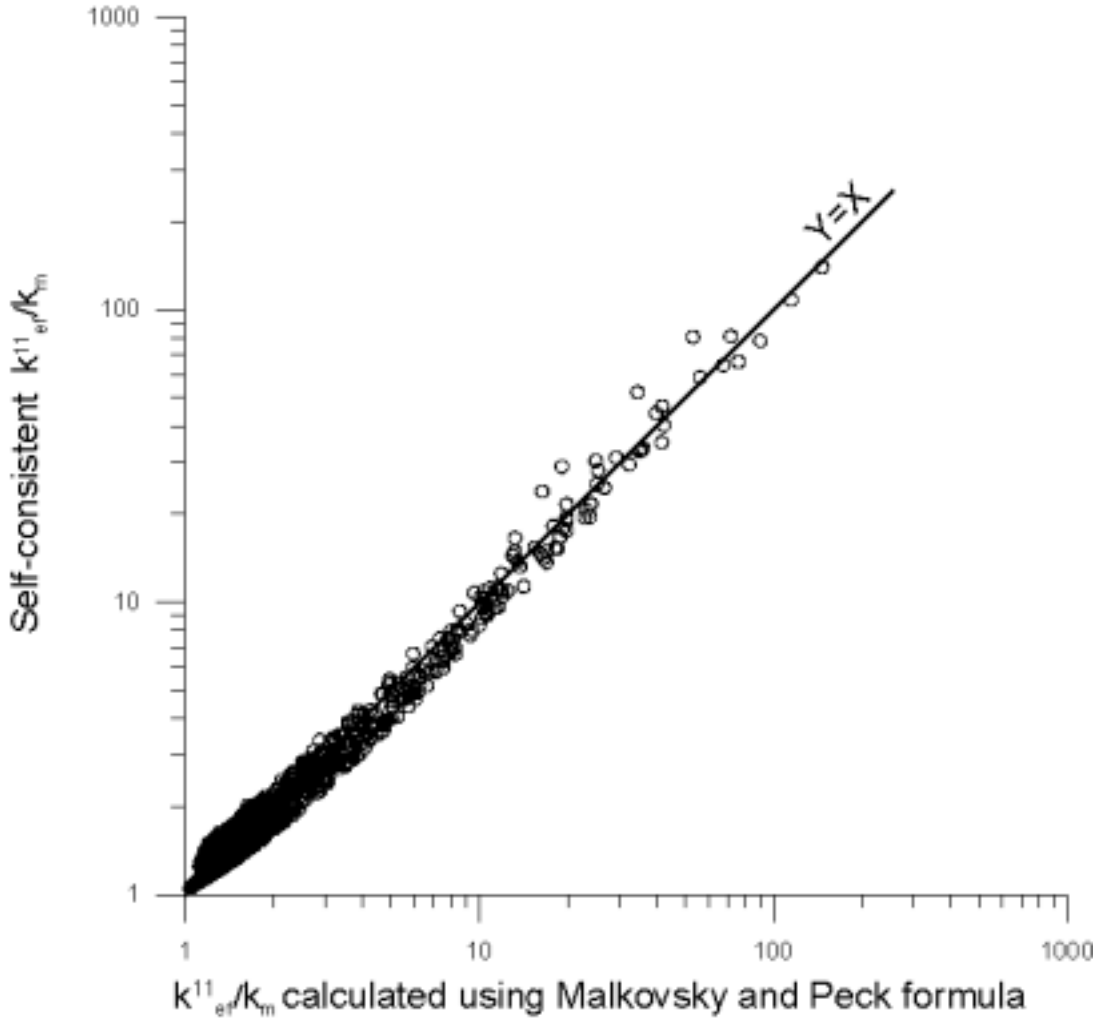
1000
100
10
1
Self-consistent k^{11}_{eff}/k_m
Y=X
1
10
100
1000
k^{11}_{eff}/k_m calculated using Malkovsky and Peck formula

Figure 5.

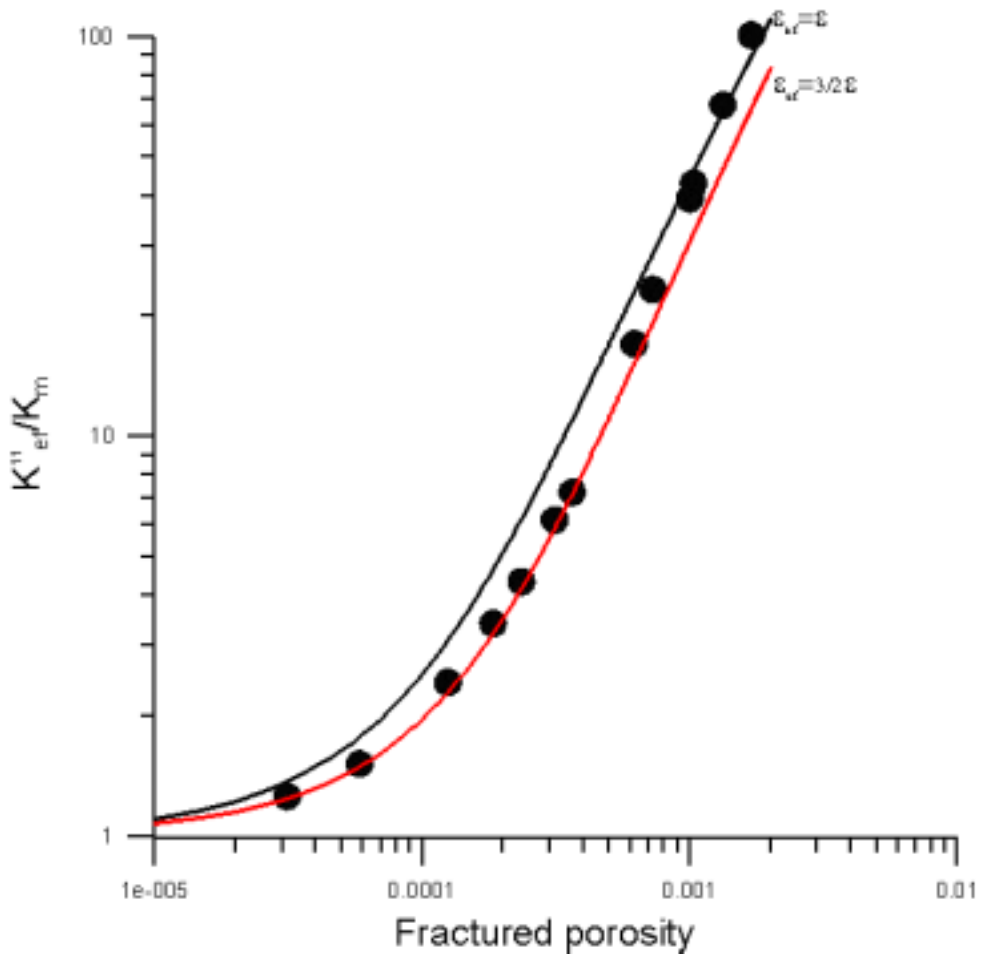
100
10
1
K''_{ef}/K_m
1e-005
0.0001
0.001
0.01
Fractured porosity
$\varepsilon_{xx}=\varepsilon$
$\varepsilon_{xx}=3/2\varepsilon$

Figure 6 .

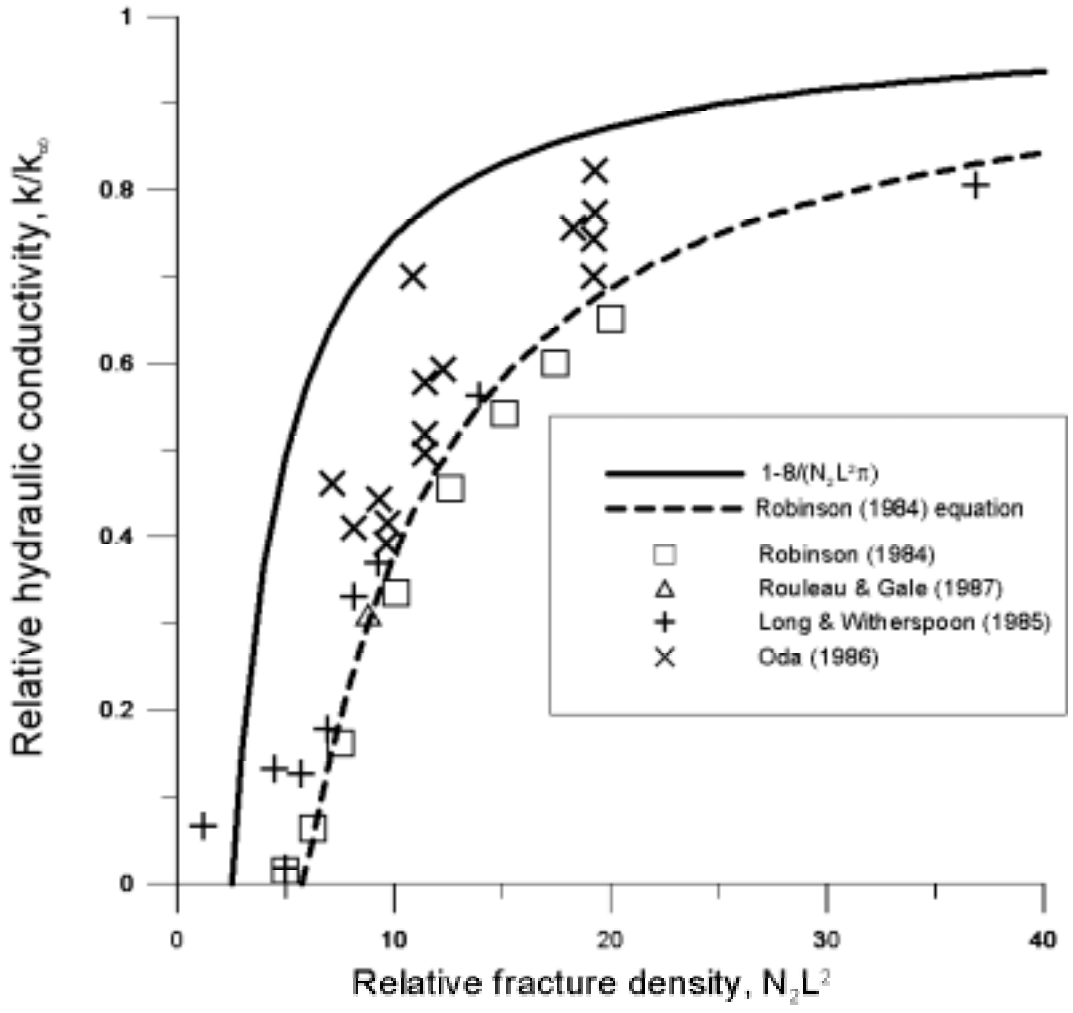
Relative hydraulic conductivity, k/k∞
Relative fracture density, N2L2
1
0.8
0.6
0.4
0.2
0
0
10
20
30
40
1-8/(N2L2π)
Robinson (1984) equation
Robinson (1984)
Rouleau & Gale (1987)
Long & Witherspoon (1985)
Oda (1986)

Figure 7.